Mathematical Biosciences and Engineering, 16(4): 2875–2905.
DOI: 10.3934/mbe.2019142
Received: 13 December 2018
Accepted: 07 March 2019
Published: 09 April 2019

http://www.aimspress.com/journal/MBE

*Research article*

# Melt flow of biopolymer through the cavities of an extruder die: Mathematical modelling

**Alexander N. Ostrikov[1], Abdymanap A. Ospanov[2,*], Vitaly N. Vasilenko[1], Nurzhan Zh. Muslimov[3], Aigul K. Timurbekova[2] and Gulnara B. Jumabekova[4]**

[1] Voronezh State University of Engineering Technologies, Voronezh, Russian Federation
[2] Kazakh National Agrarian University, Almaty, Republic of Kazakhstan
[3] Taraz innovative-humanities university, Taraz, Republic of Kazakhstan
[4] M.Kh. Dulaty Taraz State University, Taraz, Republic of Kazakhstan

* **Correspondence:** Email: obdymanap@yahoo.com, ospanov_abdymanap@mail.ru.

**Abstract:** This is an analytical solution of the two-dimensional non-isothermal mathematical model describing the change in the velocity profile of a cylindrical extrusion die. This solution is based on the following assumptions. The two-dimensional melt flow is asymmetric. A melt viscosity anomaly may take place. Heat generated by viscous friction is a factor affecting the melt flow. The melt flow moving towards the metering section is in a steady state. Neither mass forces nor inertia forces are present. Velocity gradients along the channel are neglected. The mathematical model was built up from the incompressibility equation, motion equations, energy equation, and the rheological equation. This model depicted a non-isothermal flow of rheological fluid moving through the cylindrical extrusion die. A diagram was drawn. It depicts the melt velocities at a die entrance in different cross-sectional views. Computer testing was performed to verify the obtained solutions and compare them with the real extrusion process. Difference between calculated and experimental data was below 14%. Results allow concluding a matching of numerical results with experimental data, and so the possibility of using a built-up model in an extrusion die design for single-screw extruders.

**Keywords:** mathematical modelling; extrusion; melt flow; polymer processing; die; extruder

## 1. Introduction

A problem is to improve the calculation theory and methods that are applied to extrusion equipment. If solved, it can ensure the optimal design of extruder sections for the production of food of required quality [1–4]. From this perspective, mathematical modelling of extrusion process is of critical need.

Because the quality of extruded article, as well as the extrusion machine operation, is largely dependent upon the function of a metering section, the analysis will touch upon the mathematical models of extrusion at the metering section.

A common choice for the viscosity function is the power-law equation. It is easy to make calculations of flow and stress fields with the constitutive equation of the power-law generalized Newtonian fluid. For many polymer melts, < 1 values of the power-law index correctly capture the flow behaviour at high rates of deformation [5]. The overall predictions of the power-law generalized Newtonian fluid are found to be adequate when the information about the pressure drop and the flow rate is desired. This choice is even more relevant because the target parameters in this study do not include memory effects, relaxation time, or other elasticity effects.

Based on the isothermal Newtonian flow model, James M. McKelvey derived an expression for the volumetric flow rate in the metering zone, $m^3$/sec [6]:

$$Q = F_d \cdot \frac{U_z \cdot h \cdot W}{2} - \frac{h^3 \cdot W}{12\mu_н} \cdot \left(\frac{\partial P}{\partial z}\right) \cdot F_p \cdot \tag{1}$$

Where: $Q$ –volume rate of flow in the metering zone, $m^3$/sec; $U_z$ –velocity component of barrel in z-axis direction (z-axis is oriented along the axis of a screw channel), m/sec; $h$ –screw channel depth, m; $W$ –channel width, m; $\mu_н$ –Newtonian fluid viscosity, Pa s; $\partial P/\partial z$ –pressure gradient along $z$-axis, Pa/m; $F_d$, $F_p$ –dimensionless shape factors concerning with the effect of $h/W$ on the flow ratio distribution.

Solution to this flow problem generated an equation for productivity in metering zone. However, despite the ease of solving the equation, some shortcomings do not allow getting a full picture of a melt flow through the channel in the metering zone. These shortcomings are the accepted Newtonian flow, the focus just on the problem of one-dimensional isothermal flow, the neglected convective heat transfer, the quality of extruded article, etc.

Rheological models provide the most accurate physical picture of the extrusion process [7–9]. The first close attempt to solve this problem was made by Z. Tadmor, R.V. Torner, et al. [10–12]. They introduced mathematical models for one-dimensional isothermal flow of a power-law fluid:

$$Q = \frac{V_o \cdot H \cdot |6G|^s \cdot signG}{(1+s)(2+s)} \cdot \left[(1-\lambda)|1-\lambda|^{1+s} + \lambda|\lambda|^{1+s} - (2+s)|\lambda|^{1+s}\right], \tag{2}$$

Where: $Q$ –specific volumetric flow rate, $m^3$/(sec·m); $V_o$ –velocity in the direction parallel to the moving plate, m/sec; $H$ –screw channel depth, m; $G$ –dimensionless pressure gradient; $s = 1/n$ (or $1/m$ )–reciprocal of exponent in power-law flow; sign –sign of the function $\text{sign}G = G/|G|$; $\lambda$ –dimensionless longitudinal coordinate.

$$Q = \frac{U_z \cdot h \cdot W}{2} \cdot \frac{(1-\eta_o)^{n+2} + sign\eta_o|\eta_o|^{n+2} - (n+2)|\eta_o|^{n+1}}{(1-\eta_o)^{n+1} - |\eta_o|^{n+1}} \quad (\text{in } dP/dx > 0), \tag{3}$$

Where: $Q$ –volume rate of flow, $m^3$/sec; $\eta_o$ –dimensionless coordinate with zero shear stress; $\eta_o = y_o/h$; $y_o$ –coordinate of cross-section with zero shear stress, m; $dP/dx$ –pressure gradient, Pa/m.

These models have a common drawback–no evaluation is implied for the quality of polymer melt and for the quality of extruded article, accordingly. Improving the quality of extruded article is a step essential for the improvement of processing operations. This problem can be solved by stabilising the key process parameters (volumetric flow rate, pressure, and temperature).

The problem of a polymer melt flow in single-screw extruders was considered in a range of papers with due account for the effect of melt leaking out through the gaps [9,13–14]. This resulted in an analytical expression for the volumetric flow rate in the metering zone that takes into account die leakages.

$$Q = \frac{\pi^2 \cdot D^2 \cdot N \cdot (1 - i \cdot e/S) \cdot \sin\varphi\cos\varphi \cdot (1 - \delta/h) \cdot h \cdot \psi(\eta_o)}{n+2} - \\ - \frac{B_z (n+1)^{1/n} \cdot \pi^2 D^2 N \left[ \chi (\sin\varphi)^{(n+1)/n} + (\cos\varphi)^{(n+1)/n} \right]^2 \cdot \delta^{(n+1)/n}}{6\text{tg}\varphi \cdot h^{(n+1)/n}}, \tag{4}$$

Where: $N$ –screw rotation speed, rpm; $S$ –screw pitch, m; $\varphi$ –screw helix angle; $\delta$ –flight clearance, m; $B_z$ –dimensionless pressure gradient in forward flow; $\chi$ –ratio referring to pressure gradients acting in circulation flow.

Even though viscosity anomaly was taken into account in model (4), it does not involve pressure drops in the channel and in the radial clearance.

Tadmor made the following assumptions to simplify the model. The given process is stationary. The polymer tube is uniform. The polymer travels through the channel at a constant speed. The melting point is clearly defined. The channel curvature is not a factor to consider. A melting problem is reduced to a one-dimensional problem of heat and mass transfer [12]. However, such solution does

not provide an adequate examination of convective and diffusion mechanisms of heat transfer.

Chang Dae Han suggested that the main reason for the difference between the calculated and the experimental data is the Tadmor's assumption about the infinite depth of a solid bed. According to Chang, his assumption entailed a misassessment of the temperature profile [15]. Therefore, he considered a solid bed between the barrel and the screw root. With this approach, he found the temperature distribution in the film mass (exponential law), and assumed that it does not change at melting. Hence, he was able to determine the screw temperature using the heat transfer equation.

Papers considered above are devoted to the problem of one-dimensional flow, but this approach does not allow taking into account the effect of mixing and the effect of convective heat transfer.

R.V. Torner introduced an iterative procedure of solving equations for melt in a melt zone. This practice was suggested as an addition to the already existing calculation method, which was applied to plasticizing extruders with conical units. Thus, he obtained a model of the two-dimensional non-isothermal flow of a pseudo-plastic fluid [12]:

$$Q = \frac{k(l)}{R-1} \cdot \frac{\mu_o A l_\partial b N^{1+1/n}}{\rho c_p}, \tag{5}$$

Where: $k(l)$–polytropic efficiency dependent upon the location of a cross section on the flight axis; $l$–longitudinal coordinate of standard cross section, varying within $0 \le l \le l_\partial$; $\mu_o$–material constant, Pa s; $A = (\pi \cdot D)^{1+1/n} \cdot \left[ (t - i \cdot e) / h^{1/n} \cdot Э_1 + e / \delta^{1/n} \right] \cdot i \cdot \mathrm{ctg}\phi$ ; $Э_1$ –dimensionless criterion, $Э_1 = \left[ (1-\eta_o)(\cos\varphi)^{1+1/n} + \chi(1-\eta_{ou})(\sin\varphi)^{1+1/n} \right] \cdot B_z (n+1)^{1/n}$; $\eta_{ou}$–dimensionless coordinate with zero shear stress in circulation flow; $l_\partial$–actual length of metering zone, m; $b$–temperature coefficient of viscosity, 1/deg; $R = e^{b(T-T_o)}$; $T$–melt temperature, $^o$C; $\rho$–melt density, kg/m$^3$; $c_p$–specific heat of melt, J/(kg·K).

The solution of the two-dimensional problem only cannot give the extruder characteristics that will work or a temperature profile of the melt down the screw.

V.V. Skachkov reviewed the existing methods of solving equations for melt in a melt zone [10]. The introduced parameter was the apparent melting heat. This parameter took into account that extra energy necessary to heat the melt to the average film temperature. The flow rate was found to be the strongest factor affecting the melting process; its effect was stronger than the effect of the number of rotations and effect of the barrel temperature.

Pervadchuk V.P. coined a theory of polymeric materials melting in the plasticizing extruders. According to this theory, one has to solve complete equations for the conservation of mass, momentum, and energy [16–17]. Piecewise constant approximation of changes in longitudinal velocity allows reducing the solution of the three-dimensional stationary problem to the two-dimensional non-stationary one. The qualitatively new characteristics of melting were obtained. By

qualitatively new, one should understand the shape of a solid film mass, velocity and temperature profiles, etc. However, the problem that was solved applies only to the Newtonian fluid and to a constant screw channel height.

Therefore, in the single-screw extrusion, one of the most important issues is to build a mathematical model that would allow him/her to predict the quality of extruded article and to take into account the required quality indicators when calculating or selecting the geometry of a screw. Yet, melt behaviour in the forming channels of a die and in the metering section is insufficiently studied. Therefore, it is essential to build mathematical models of extrusion that would describe the change in temperature/pressure and in the average velocity of the fluid travel in the zone. This necessity rises from the fact that these parameters have the direct effect on the quality of a finished product and on the quality of the extruder operation.

The purpose of this article is to present an analytical solution to the two-dimensional non-isothermal mathematical model describing the change in velocity profile of a cylindrical extrusion die.

## 2. Materials and methods

Rheological melt flow is pushed through the channel to the metering section of a die, and then it is pressed out through the die cavities. To study the melt flow in the cavity of a die, let us consider the flow of a fluid in a stepped cylindrical channel (dimensions: length $l_1$ and diameter $d_1$; length $l_2$ and diameter $d_2$. $d_1 > d_2$). Let the melt flow in the die body to be known and stationary.

Extrusion process was investigated on grain crops in the single-screw extruder KMZ (Figure 1).

The investigation over complex mixtures was performed using the experimental single screw extruder EUM-1 (Figure 2).

To assess the nature of changes that occur in the structure of material at extrusion, the focus was laid on the qualitative changes that emerge in crops along the work chamber of the single-screw extruder (Figure 3).

The pre-moistened raw material enters the feed section, where it is mixed to thickening. When this happens, air between the particles of the product is squeezed out to some extent. In the feed section, coarse-grained particles have voids between them. In the compression section, particles are under significant mechanical stress that causes them to deform throughout the volume. At the same time, internal stress increases in a stepwise manner. When it reaches the point above the compressive strength, the fracture of biopolymers and cellular particles becomes stronger, enabling the compaction and the beginning of melt formation.

In the homogenization zone, a homogeneous melt is formed with a small number of particles that have not yet melted.

In the metering section, which has the pressure stabilisation and pressurization function, with temperature maintained at 120 to 190 ℃, the product becomes plastic (homogenization completed). The insignificant traces of unmelted starch kernel are associated with the incomplete denaturation of protein molecules, especially globular ones. Thus, the properties of an extruded product depend on both the starch phase and the protein phase. The product that came out of the extruder was porous, with a slight decrease in mechanical strength.

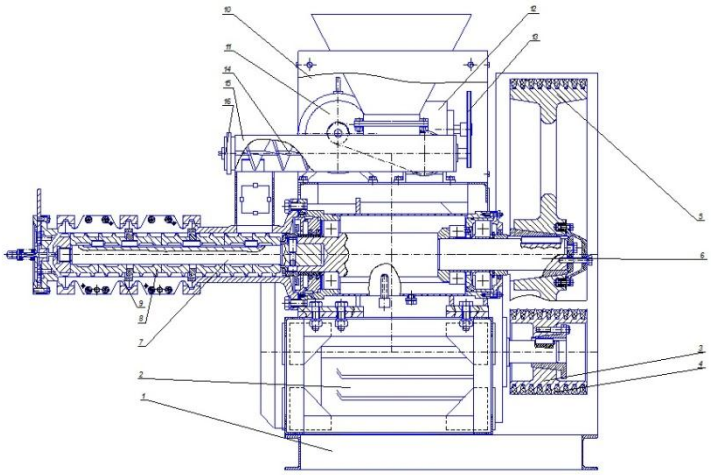

**Figure 1.** KMZ-2U extruder chart: 1–base; 2–motor; 3–driver pulley; 4–belt; 5–driven pulley; 6–shaft; 7–stud; 8–flight; 9–body; 10–frame; 11–feed drive motor; 12–gearbox; 13–chain drive; 14–drive feed screw; 15–housing; 16–bearing assembly.

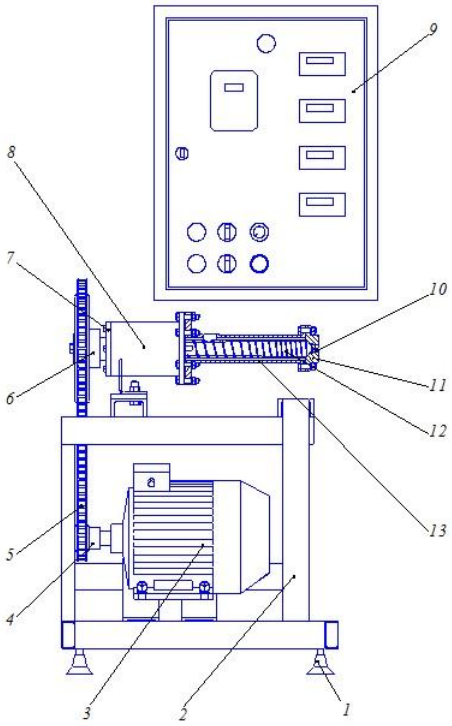


**Figure 2.** EUM-1 extruder chart: 1–adjustable base leg; 2–frame; 3–motor; 4–drive sprocket; 5–chain; 6–driven sprocket; 7–bearing cover; 8–bearing body; 9–control cabinet; 10–die head; 11–die body; 12–screw; 13–work chamber.

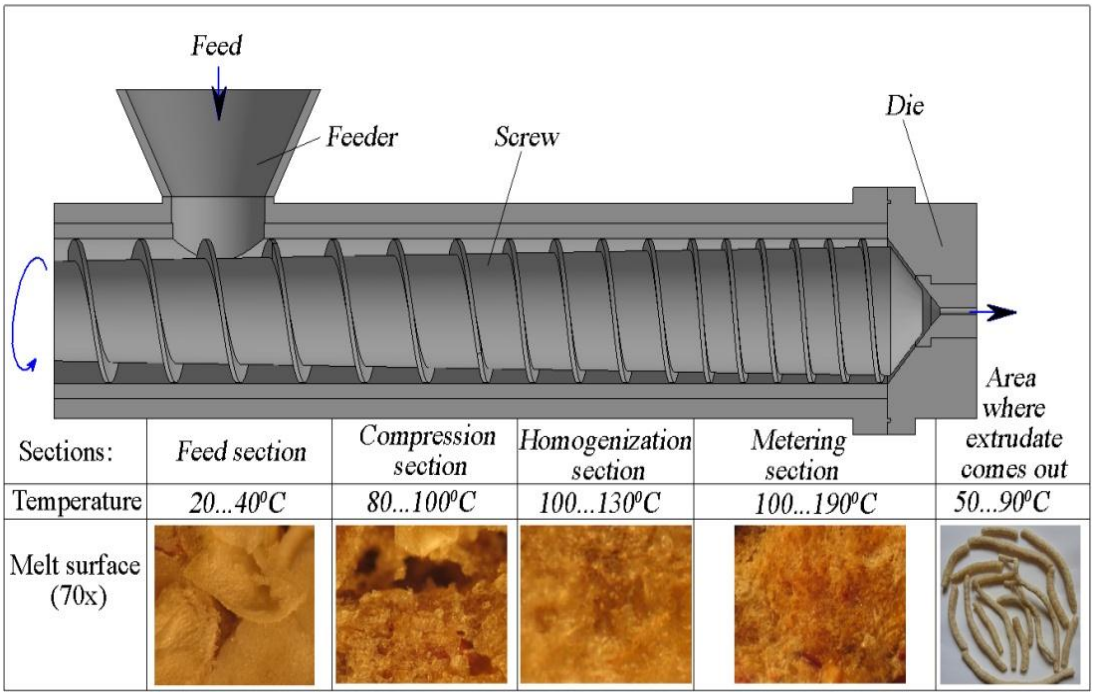


**Figure 3.** The pattern of product transformation at extrusion.

Histological studies of the extruded material structure revealed that in the heating zone, where the heating elements are located, physicochemical parameters of initial mixtures did not significantly change. Large particles were dense, with uneven edges, while smaller particles were more spherical in shape.

A system of differential equations for non-isothermal flow can be applied to each *k*-th channel. For an asymmetric flow, modelled as the two-dimensional flow, tangential velocity component equals to zero. Because the melt flow is stationary, the viscosity anomaly is present, and the melt itself is incompressible, the differential equations (if small mass forces are ignored) can be written in the cylindrical coordinate system as:

Incompressibility equation [13]:

$$\frac{\partial \vartheta_z}{\partial z} + \frac{\vartheta_r}{r} + \frac{\partial \vartheta_r}{\partial r} = 0, \tag{6}$$

Motion equation:

$$\rho\left(\vartheta_r \frac{\partial \vartheta_r}{\partial r} + \vartheta_z \frac{\partial \vartheta_r}{\partial z}\right) = -\frac{\partial p}{\partial r} + 2\frac{\partial}{r\partial r}\left(r\eta \frac{\partial \vartheta_r}{\partial r}\right) + \frac{\partial}{\partial z}\left[\eta\left(\frac{\partial \vartheta_r}{\partial z} + \frac{\partial \vartheta_z}{\partial r}\right)\right] - 2\eta\frac{\vartheta_r}{r^2}, \tag{7}$$

$$\rho\left(\vartheta_r \frac{\partial \vartheta_z}{\partial r} + \vartheta_z \frac{\partial \vartheta_z}{\partial z}\right) = -\frac{\partial p}{z} + 2\frac{\partial}{\partial z}\left(\eta \frac{\partial \vartheta_z}{\partial z}\right) + \frac{1}{r}\frac{\partial}{\partial r}\left[r\eta\left(\frac{\partial \vartheta_r}{\partial z} + \frac{\partial \vartheta_z}{\partial r}\right)\right], \tag{8}$$

Energy equation:

$$\rho c\left(\vartheta_z \frac{\partial T}{\partial z}+\vartheta_r \frac{\partial T}{\partial r}\right)=\frac{\partial}{\partial z}\left(\lambda \frac{\partial T}{\partial z}\right)+\frac{1}{r}\frac{\partial}{\partial r}\left(r\lambda \frac{\partial T}{\partial r}\right)+\Phi, \tag{9}$$

Where: $\Phi$–dissipation function, characterizing the conversion of kinetic energy into heat energy:

$$\Phi=\tau_{zz}\frac{\partial \vartheta_z}{\partial z}+\tau_{rr}\frac{\partial \vartheta_r}{\partial r}+\tau_{\theta\theta}\frac{\vartheta_r}{r}+\tau_{2r}\left(\frac{\partial \vartheta_z}{\partial r}+\frac{\partial \vartheta_r}{\partial \tau}\right), \tag{10}$$

Where: $\tau_{zz}=2\eta(I_2,T)\frac{\partial \vartheta_z}{\partial z}$; $\tau_{rr}=2\eta(I_2,T)\frac{\partial \vartheta_r}{\partial r}$; $\tau_{\theta\theta}=2\eta(I_2,T)\frac{\vartheta_r}{r}$;

$\tau_{zr}=\tau_{rz}=\eta(I_2,T)\left(\frac{\partial \vartheta_r}{\partial z}+\frac{\partial \vartheta_z}{\partial r}\right)$–stress tensor components.

For a continuous flow, a rheological equation was used, expressed through a generalized power law:

$$\eta=\eta_o\, e^{-\beta(T-T_o)}\left(\frac{I_2}{2}\right)^{\frac{m-1}{2}}, \tag{11}$$

Where: $\eta_o$, $m$–material constants; $\beta$–temperature coefficient of viscosity; $I_2$–quadratic strain rate tensor,

$$\frac{I_2}{2}=2\left[\left(\frac{\partial \vartheta_z}{\partial z}\right)^2+\left(\frac{\partial \vartheta_r}{\partial r}\right)^2+\left(\frac{\vartheta_r}{r}\right)^2\right]+\left(\frac{\partial \vartheta_r}{\partial z}+\frac{\partial \vartheta_z}{\partial r}\right)^2,. \tag{12}$$

To reduce the order, (1)–(7) were expressed as the alternating current $\varphi$

$$\vartheta_z=\frac{1}{r\rho}\frac{\partial \psi}{\partial r};\quad \vartheta_r=-\frac{1}{r\rho}\frac{\partial \psi}{\partial z}, \tag{13}$$

and vorticity $\omega$:

$$\omega=\frac{\partial \vartheta_r}{\partial z}-\frac{\partial \vartheta_z}{\partial r}. \tag{14}$$

Then, incompressibility Eq (1) will be accomplished automatically.

Let us transform motion equations using vorticity and current variables. For this purpose, Eq (7) was differentiated with respect to *z*, and Eq (8)–with respect to *r*. Results from the differentiation of Eq (8) was subtracted from the results that were obtained in differentiation of Eq (7).

Expression on the left of (6) will be:

$$\frac{\partial}{\partial z}\left[\rho\left(\vartheta_r\frac{\partial\vartheta_r}{\partial r}+\vartheta_z\frac{\partial\vartheta_r}{\partial z}\right)\right]=\rho\left[\frac{\partial\vartheta_r}{\partial z}\frac{\partial\vartheta_r}{\partial r}+\vartheta_r\frac{\partial^2\vartheta_r}{\partial r\partial z}+\frac{\partial\vartheta_z}{\partial z}\frac{\partial\vartheta_r}{\partial z}+\vartheta_z\frac{\partial^2\vartheta_r}{\partial z^2}\right], \quad (15)$$

$$\frac{\partial}{\partial r}\left[\rho\left(\vartheta_r\frac{\partial\vartheta_z}{\partial r}+\vartheta_z\frac{\partial\vartheta_z}{\partial z}\right)\right]=\rho\left[\frac{\partial\vartheta_z}{\partial r}\frac{\partial\vartheta_r}{\partial z}+\vartheta_z\frac{\partial^2\vartheta_r}{\partial r\partial z}+\frac{\partial\vartheta_z}{\partial z}\frac{\partial\vartheta_r}{\partial z}+\vartheta_r\frac{\partial^2\vartheta_r}{\partial r^2}\right]. \quad (16)$$

By subtracting (15) from (16), one will get:

$$\rho\left[\vartheta_r\left(\frac{\partial^2\vartheta_r}{\partial r\partial z}-\frac{\partial^2\vartheta_z}{\partial r^2}\right)+\vartheta_z\left(\frac{\partial^2\vartheta_r}{\partial z^2}-\frac{\partial^2\vartheta_z}{\partial r\partial z}\right)+\frac{\partial\vartheta_r}{\partial r}\left(\frac{\partial\vartheta_r}{\partial z}-\frac{\partial\vartheta_z}{\partial r}\right)+\frac{\partial\vartheta_z}{\partial z}\left(\frac{\partial\vartheta_r}{\partial z}-\frac{\partial\vartheta_z}{\partial r}\right)\right]=$$

$$=\rho\left[\vartheta_r\frac{\partial\omega}{\partial r}+\vartheta_z\frac{\partial\omega}{\partial z}+\left(\frac{\partial\vartheta_r}{\partial r}+\frac{\partial\vartheta_z}{\partial z}\right)\omega\right]=\left[\frac{\partial}{\partial z}\left(\frac{\omega}{r}\frac{\partial\psi}{\partial r}\right)-\frac{\partial}{\partial r}\left(\frac{\omega}{r}\frac{\partial\psi}{\partial z}\right)\right]. \quad (17)$$

Expressions on the right of (6) and (7) were done by analogy:

$$\Re=\frac{\partial}{z}\left\{-\frac{\partial P}{\partial r}+2\frac{\partial}{r\partial r}\left(r\eta\frac{\partial\vartheta_r}{\partial r}\right)+\frac{\partial}{\partial z}\left[\eta\left(\frac{\partial\vartheta_r}{\partial z}+\frac{\partial\vartheta_z}{\partial r}\right)\right]-2\eta\frac{\vartheta_r}{r^2}\right\}-$$

$$-\frac{\partial}{\partial r}\left\{-\frac{\partial P}{\partial z}+2\frac{\partial}{\partial z}\left(\eta\frac{\partial\vartheta_z}{\partial z}\right)+\frac{\partial}{\partial r}\left[r\eta\left(\frac{\partial\vartheta_r}{\partial z}+\frac{\partial\vartheta_z}{\partial r}\right)\right]\right\}=$$

$$=\frac{\partial}{\partial z}\left\{\frac{2}{r}\eta\frac{\partial\vartheta_r}{\partial r}+2\frac{\partial\eta}{\partial r}\frac{\partial\vartheta_r}{\partial r}+2\eta\frac{\partial^2\vartheta_r}{\partial r^2}+\frac{\partial\eta}{\partial z}\frac{\partial\vartheta_r}{\partial z}+\eta\frac{\partial^2\vartheta_r}{\partial z^2}+\frac{\partial\eta}{\partial r}\frac{\partial\vartheta_z}{\partial r}+\eta\frac{\partial^2\vartheta_z}{\partial r\partial z}-2\eta\frac{\vartheta_r}{r^2}\right\}-$$

$$-\frac{\partial}{\partial r}\left\{\frac{1}{r}\eta\frac{\partial\vartheta_r}{\partial z}+\frac{1}{r}\eta\frac{\partial\vartheta_z}{\partial r}+\frac{\partial\eta}{\partial r}\frac{\partial\vartheta_r}{\partial z}+\frac{\partial\eta}{\partial r}\frac{\partial\vartheta_z}{\partial r}+\eta\frac{\partial^2\vartheta_r}{\partial r\partial z}+\eta\frac{\partial^2\vartheta_z}{\partial r^2}+2\frac{\partial\eta}{\partial z}\frac{\partial\vartheta_z}{\partial z}+2\eta\frac{\partial^2\vartheta_z}{\partial z^2}\right\}=$$

$$=\frac{2}{r}\frac{\partial\eta}{\partial z}\frac{\partial\vartheta_r}{\partial r}+\frac{2}{r}\eta\frac{\partial^2\vartheta_r}{\partial r\,dz}+2\frac{\partial^2\eta}{\partial r\partial z}\frac{\partial\vartheta_r}{\partial r}+2\frac{\partial\eta}{\partial r}\frac{\partial^2\vartheta_r}{\partial r\,dz}+2\frac{\partial\eta}{\partial z}\frac{\partial^2\vartheta_r}{\partial r^2}+2\eta\frac{\partial}{\partial z}\left(\frac{\partial^2\vartheta_r}{\partial r^2}\right)+$$

$$+\frac{\partial^2\eta}{\partial z^2}\frac{\partial\vartheta_r}{\partial z}+\frac{\partial\eta}{\partial z}\frac{\partial^2\vartheta_r}{\partial z^2}+\frac{\partial\eta}{\partial z}\frac{\partial^2\vartheta_r}{\partial z^2}+\eta\frac{\partial}{\partial z}\left(\frac{\partial^2\vartheta_r}{\partial z^2}\right)+\frac{\partial^2\eta}{\partial z^2}\frac{\partial\vartheta_z}{\partial r}+\frac{\partial\eta}{\partial z}\frac{\partial^2 z}{\partial r\partial z}+$$

$$+\frac{1}{r^2}\eta\frac{\partial\vartheta_r}{\partial z}-\frac{1}{r}\frac{\partial\eta}{\partial r}\frac{\partial\vartheta_r}{\partial z}-\frac{1}{r}\eta\frac{\partial^2\vartheta_u}{\partial r\partial z}+\frac{1}{r^2}\eta\frac{\partial\vartheta_z}{\partial r}-\frac{1}{r}\frac{\partial\eta}{\partial r}\frac{\partial\vartheta_z}{\partial r}-\frac{1}{r}\eta\frac{\partial^2\vartheta_z}{\partial r^2}-$$

$$-\frac{\partial^2\eta}{\partial r^2}\frac{\partial \vartheta_r}{\partial z}-\frac{\partial\eta}{\partial r}\frac{\partial^2\vartheta_r}{\partial z\partial r}-\frac{\partial^2\eta}{\partial r^2}\frac{\partial\vartheta_z}{\partial r}-\frac{\partial\eta}{\partial r}\frac{\partial^2\vartheta_z}{\partial r^2}-\frac{\partial\eta}{\partial r}\frac{\partial^2\vartheta_r}{\partial z\partial r}-\eta\frac{\partial}{\partial z}\left(\frac{\partial^2\vartheta_r}{\partial r^2}\right)-$$

$$-\frac{\partial\eta}{\partial r}\frac{\partial^2\vartheta_z}{\partial r^2}-\eta\frac{\partial}{\partial r}\left(\frac{\partial^2\vartheta_z}{\partial r^2}\right)-2\frac{\partial^2\eta}{\partial r\partial z}\frac{\partial\vartheta_z}{\partial z}-2\frac{\partial\eta}{\partial z}\frac{\partial^2\vartheta_z}{\partial r\partial z}-2\frac{\partial\eta}{\partial r}\frac{\partial^2\vartheta_z}{\partial z^2}-2\eta\frac{\partial}{\partial r}\left(\frac{\partial^2\vartheta_z}{\partial z^2}\right) \tag{18}$$

Equation (18) was transformed by grouping:

$$\Re=\frac{\eta}{r^2}\left\{\frac{\partial}{\partial r}\left[r^3\frac{\partial}{\partial r}\left(\frac{\omega}{r}\right)\right]+\frac{\partial}{\partial z}\left[r^3\frac{\partial}{\partial z}\left(\frac{\omega}{r}\right)\right]\right\}+S_\omega \tag{19}$$

Where:

$$S_\omega=\frac{2}{r}\frac{\partial\eta}{\partial z}\frac{\partial\vartheta_r}{\partial r}+2\frac{\partial^2\eta}{\partial r\partial z}\frac{\partial\vartheta_r}{\partial r}+2\frac{\partial\eta}{\partial r}\frac{\partial^2\vartheta_r}{\partial r\partial z}+2\frac{\partial\eta}{\partial z}\frac{\partial^2\vartheta_r}{\partial r^2}+\frac{\partial^2\eta}{\partial z^2}\frac{\partial\vartheta_r}{\partial z}+2\frac{\partial\eta}{\partial z}\frac{\partial^2\vartheta_r}{\partial z^2}+$$

$$+\frac{\partial^2\eta}{\partial z^2}\frac{\partial\vartheta_z}{\partial r\partial z}+2\frac{\partial\eta}{\partial z}\frac{\partial^2\vartheta_z}{\partial r\partial z}-2\frac{\partial\eta}{\partial r}\frac{\vartheta_r}{r^2}-\frac{1}{r}\frac{\partial\eta}{\partial r}\frac{\partial\vartheta_r}{\partial z}-\frac{1}{r}\frac{\partial\eta}{\partial r}\frac{\partial\vartheta_z}{\partial r}-\frac{\partial^2\eta}{\partial r^2}\frac{\partial\vartheta_r}{\partial z}-\frac{\partial\eta}{\partial r}\frac{\partial^2\vartheta_r}{\partial r\partial z}-$$

$$-\frac{\partial^2\eta}{\partial r^2}\frac{\partial\vartheta_z}{\partial r}-2\frac{\partial\eta}{\partial r}\frac{\partial^2\vartheta_z}{\partial r^2}-\frac{\partial\eta}{\partial r}\frac{\partial^2\vartheta_r}{\partial r\partial z}-2\frac{\partial^2\eta}{\partial r\partial z}\frac{\partial\vartheta_z}{\partial z}-2\frac{\partial\eta}{\partial z}\frac{\partial\vartheta_z^2}{\partial r\partial z}-2\frac{\partial\eta}{\partial r}\frac{\partial^2\vartheta_z}{\partial z^2} \tag{20}$$

Thus, in current and vorticity coordinates, motion equation will take the following form:

$$\frac{\partial}{\partial z}\left(\frac{\omega}{r}\frac{\partial\psi}{\partial r}\right)-\frac{\partial}{\partial r}\left(\frac{\omega}{r}\frac{\partial\psi}{\partial z}\right)=\frac{\eta}{r^2}\left\{\frac{\partial}{\partial r}\left[r^3\frac{\partial}{\partial r}\left(\frac{\omega}{r}\right)\right]+\frac{\partial}{\partial z}\left[r^3\frac{\partial}{\partial z}\left(\frac{\omega}{r}\right)\right]\right\}+S_\omega, \tag{21}$$

Where: $S_\omega$ is determined by (20).

In new coordinates, energy equation will be as follows:

$$\frac{c}{r}\left(\frac{\partial\psi}{\partial r}\frac{\partial T}{\partial z}-\frac{\partial\psi}{\partial z}\frac{\partial T}{\partial r}\right)=\lambda\left(\frac{\partial^2T}{\partial z^2}+\frac{1}{r}\frac{\partial}{\partial r}\left(r\frac{\partial T}{\partial r}\right)\right)+\Phi, \tag{22}$$

Where:

$$\Phi=\eta\frac{I_2}{2};\ \frac{I_2}{2}=2\left[\left(\frac{1}{\rho r^2}\frac{\partial\psi}{\partial z}-\frac{1}{\rho r}\frac{\partial^2\psi}{\partial z\partial r}\right)^2+\left(\frac{1}{\rho r^2}\frac{\partial\psi}{\partial z}\right)^2+\left(\frac{1}{\rho r}\frac{\partial^2\psi}{\partial z\partial r}\right)^2\right]+$$

$$+\left(\frac{1}{\rho r}\frac{\partial^2\psi}{\partial r^2}-\frac{1}{\rho r^2}\frac{\partial\psi}{\partial r}-\frac{1}{\rho r}\frac{\partial^2\psi}{\partial z^2}\right)=$$

$$=\frac{1}{\rho^2 r^2}\left\{2\left[\left(\frac{1}{r}\frac{\partial\psi}{\partial z}-\frac{\partial^2\psi}{\partial z\,\partial r}\right)^2+\left(\frac{1}{r}\frac{\partial\psi}{\partial z}\right)^2+\left(\frac{\partial^2\psi}{\partial z\,\partial r}\right)^2\right]+\left(\frac{\partial^2\psi}{\partial r^2}-\frac{1}{r}\frac{\partial\psi}{\partial r}-\frac{\partial^2\psi}{\partial z^2}\right)^2\right\}.$$

Equations (19) and (22) were complemented by equation for vorticity $\omega$, which in a cylindrical coordinate system:

$$\frac{\partial}{\partial z}\left(\frac{1}{\rho r}\frac{\partial\psi}{\partial z}\right)+\frac{\partial}{\partial r}\left(\frac{1}{\rho r}\frac{\partial\psi}{\partial r}\right)+\omega=0. \tag{23}$$

Thus, a system was built up from three Eqs (19), (22) and (23)—equations for current $\psi$, vorticity $\omega$ and temperature $T$ that require boundary conditions:

$$\vartheta_r\big|_{z=0}=0,\ \vartheta_z\big|_{z=0}=\vartheta_0, \tag{24}$$

$$\vartheta_r\big|_{r=R}=0,\ \vartheta_z\big|_{r=R}=\vartheta_0, \tag{25}$$

$$T\big|_{r=R}=T_0, \tag{26}$$

Where: $T_0$–barrel wall temperature, $v_0$ – inlet velocity.

Initial melt temperature is assumed to be distributed across the cross-section uniformly and to be equal to $T_0$

$$T\big|_{z=0}=T_0,\ P\big|_{z=0}=P_0. \tag{27}$$

Aside from that, symmetry condition was given for functions $\vartheta_z$, $\vartheta_r$, and $T$:

$$\left.\frac{\partial\vartheta_r}{\partial r}\right|_{r=0}=\left.\frac{\partial\vartheta_z}{\partial r}\right|_{r=0}=\left.\frac{\partial T}{\partial r}\right|_{r=0}=0. \tag{28}$$

For current and vorticity variables in (24–28), conditions are as follows:

At channel inlet

$$\psi\big|_{z=0}=\frac{\vartheta_0\rho r^2}{2},\ \omega\big|_{z=0}=0,\ T\big|_{z=0}=T_0; \tag{29}$$

At inside barrel wall

$$T\big|_{r=R_э} = T_0,\ \psi\big|_{r=R_э} = 0. \tag{30}$$

For vorticity, boundary condition can be determined from equation for a current:

$$-\rho R_э \omega\big|_{r=R_э} = \left.\frac{\partial^2 \psi}{\partial r^2}\right|_{r=R_э} \tag{31}$$

It was assumed true for the zone before the boundary.

To determine vorticity at the boundary, $\left.\frac{\partial \psi}{\partial r}\right|_{r=\mathrm{Re}} = 0$ condition of melt adhesion should be met. This can be accomplished using a finite difference scheme for a system of equations:

Conditions along the axis of symmetry

$$\left.\frac{\partial T}{\partial r}\right|_{r=0} = 0, \qquad \psi\big|_{r=0} = 0, \qquad \omega\big|_{r=0} = 0. \tag{32}$$

With new variables

$$\overline{r} = r / R_э,\ \overline{z} = z / R_э, \tag{33}$$

and with new values of velocity $\vartheta_0$, pressure $P_0$, temperature $T_0$ and viscosity $\eta_0$, dimensionless values

$$\overline{\psi} = \frac{\psi}{\vartheta_0 R_э^2 \rho},\ \overline{\omega} = \frac{\omega R_э}{\vartheta_0},\ \overline{T} = \frac{T}{T_0},\ \overline{\eta} = \frac{\eta}{\eta_0} \tag{34}$$

can be determined.

With (33) and (34), Eqs (21) and (22) and boundary conditions (29)–(32) can be written in a dimensionless form:

Equation for a current function (general equation of motion)

$$\frac{\partial}{\partial \overline{z}}\left(\frac{\overline{\omega}}{\overline{r}}\frac{\partial \overline{\psi}}{\partial \overline{r}}\right) - \frac{\partial}{\partial \overline{r}}\left(\frac{\overline{\omega}}{\overline{r}}\frac{\partial \overline{\psi}}{\partial \overline{z}}\right) = \frac{\vec{\eta}}{\overline{r}^2\, Re}\left\{\frac{\partial}{\partial \overline{r}}\left[\overline{r}^3 \frac{\partial}{\partial \overline{r}}\left(\frac{\overline{\omega}}{\overline{r}}\right)\right] + \frac{\partial}{\partial \overline{z}}\left[\overline{r}^3 \frac{\partial}{\partial \overline{z}}\left(\frac{\overline{\omega}}{\overline{r}}\right)\right]\right\} + \overline{S}_\omega; \tag{35}$$

Where:

$$\overline{S}_\omega = \frac{R_э^2}{\vartheta_0^2 \rho} S_\omega, \tag{36}$$

energy equation

$$\frac{1}{\bar{r}}\left(\frac{\partial\overline{\psi}}{\partial\bar{r}}\frac{\partial\overline{T}}{\partial\bar{z}}-\frac{\partial\overline{\psi}}{\partial\bar{z}}\frac{\partial\overline{T}}{\partial\bar{r}}\right)=\frac{1}{Pe}\left(\frac{\partial^2\overline{T}}{\partial\bar{z}^2}+\frac{1}{\bar{r}}\frac{\partial}{\partial\bar{r}}\left(\bar{r}\frac{\partial\overline{T}}{\partial\bar{r}}\right)\right)+\overline{\Phi}; \tag{37}$$

vorticity equation

$$\frac{\partial}{\partial\bar{z}}\left(\frac{1}{\bar{r}}\frac{\partial\overline{\psi}}{\partial\bar{z}}\right)+\frac{\partial}{\partial\bar{r}}\left(\frac{1}{\bar{r}}\frac{\partial\overline{\psi}}{\partial\bar{r}}\right)+\overline{\omega}=0 \tag{38}$$

temperature boundary conditions

$$\overline{T}\big|_{\bar{z}=0}=1,\quad \overline{T}\big|_{\bar{r}=1}=1; \tag{39}$$

current boundary conditions

$$\psi\big|_{z=0}=\frac{\bar{r}^2}{2}; \tag{40}$$

$$\psi\big|_{r=1}=\frac{1}{2}; \tag{41}$$

vorticity boundary conditions

$$-\overline{\omega}\big|_{r=1}=\left.\frac{\partial^2\psi}{\partial\bar{r}^2}\right|_{r=1}; \tag{42}$$

conditions along the axis of symmetry

$$\left.\frac{\partial\overline{T}}{\partial\bar{r}}\right|_{\bar{r}=0}=0,\quad \overline{\psi}\big|_{\bar{r}=0}=0,\quad \overline{\omega}\big|_{\bar{r}=0}=0. \tag{43}$$

Thus, a mathematical model was built for a non-isothermal flow of rheological fluid in a cylindrical channel. Expressions assume $Re=\vartheta_0 R_э\rho/\eta_0$ (Reynolds number); $Ec=\vartheta_0^2/(T_0 c)$ (Eckert's number); $Pe=\rho c\vartheta_0 R_э/\lambda$ (Peclet number).

In (37), function $\overline{\Phi}$ is as follows:

$$\overline{\Phi}\left(\overline{\psi},\,\overline{T},\,\bar{z},\,\bar{r}\right)=\frac{Ec}{Re}\overline{\eta}\left(\frac{\bar{I}_2}{2}\right), \tag{44}$$

Where:

$$\frac{\bar{I}_2}{2}=\frac{1}{\bar{r}}\left\{2\left[\left(\frac{1}{\bar{r}}\frac{\partial\bar{\psi}}{\partial\bar{z}}-\frac{\partial^2\bar{\psi}}{\partial\bar{z}\,\partial\bar{r}}\right)^2+\left(\frac{1}{\bar{r}}\frac{\partial\bar{\psi}}{\partial\bar{z}}\right)^2+\left(\frac{\partial^2\bar{\psi}}{\partial\bar{z}\,\partial\bar{r}}\right)^2\right]+\left(\frac{\partial^2\bar{\psi}}{\partial\bar{r}^2}-\frac{1}{\bar{r}}\frac{\partial\bar{\psi}}{\partial\bar{r}}-\frac{\partial^2\bar{\psi}}{\partial\bar{z}^2}\right)^2\right\}, \quad (45)$$

$$\bar{\eta}=e^{-\beta T_0\left(\bar{T}-1\right)}\left(\frac{\vartheta_0^2\bar{I}_2}{R_э^2\,2}\right)^{\frac{m-1}{2}}. \quad (46)$$

In Eq (35), $\bar{S}_\omega$ function is nonlinear and contains terms with first and second order derivatives of viscosity function $\eta$ that characterizes viscosity profile of the melt. The structure of $\bar{S}_\omega$ function can be selected by modelling the melt flow in the channel using (35)–(43).

When fluid flows out of an adapter channel with a larger diameter into a die cavity of a smaller diameter, a flow forms at a relatively large distance before entering the die. With a certain velocity profile, fluid flow that is entering the metering section transforms into a parabolic one in a stepwise fashion. It is a common case when the melt accumulates in dead spots and flows in circulatory motion, forming vortices.

As can be seen from the mathematical model (35)–(43), process patterns depend on many parameters: Rheological characteristics of melt, channel size, and geometry, thermal, physical and hydraulic properties of the melt, and parameters affecting the process flow (boundary and initial conditions). The flow rate profiles of the melt at a die exit can also be calculated.

Because the mathematical model of a melt flow includes (35)–(43), the finite difference method was applied for numerical implementation. This method was the one settled on because the analytical solution is very difficult to generate and numerical methods are applied mainly to rheological melts [13–14,18].

With the axis of symmetry of the channel, the following system can be drawn (Figure 1).

Figure 4 depicts some channel that is followed by the die inlet. This channel has some radius $R_c$ and some length $L_c$. To analyze the formation of dead spots near the die, we assumed that the velocity profile of a melt flow in the section is uniform. Such an approach can be applied if the condition $R_c >> R_d$ (3–5-fold, approximately) is met [7–8,19].

The problem-solving algorithm was considered on a uniform grid. Some domain $D$ was gridded uniformly (grid step $H_z$ and $H_R$ with respect to $z$ and $R$, respectively) (Figure 5).

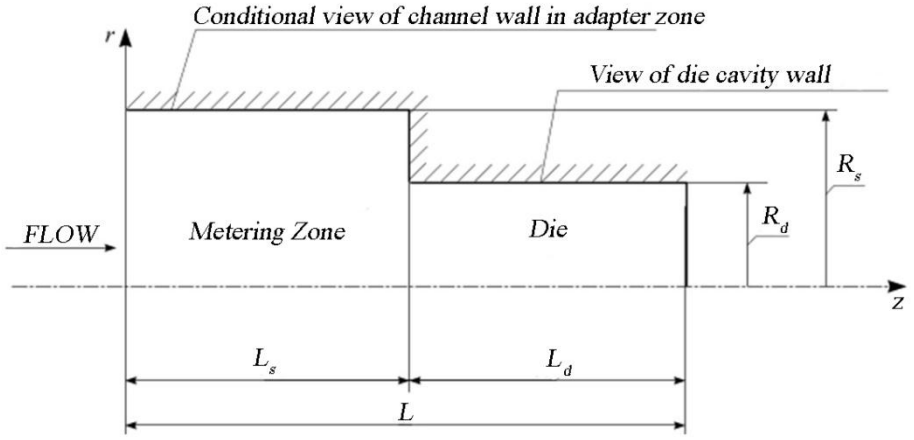


**Figure 4.** The melt flow formation in the metering section: A model.

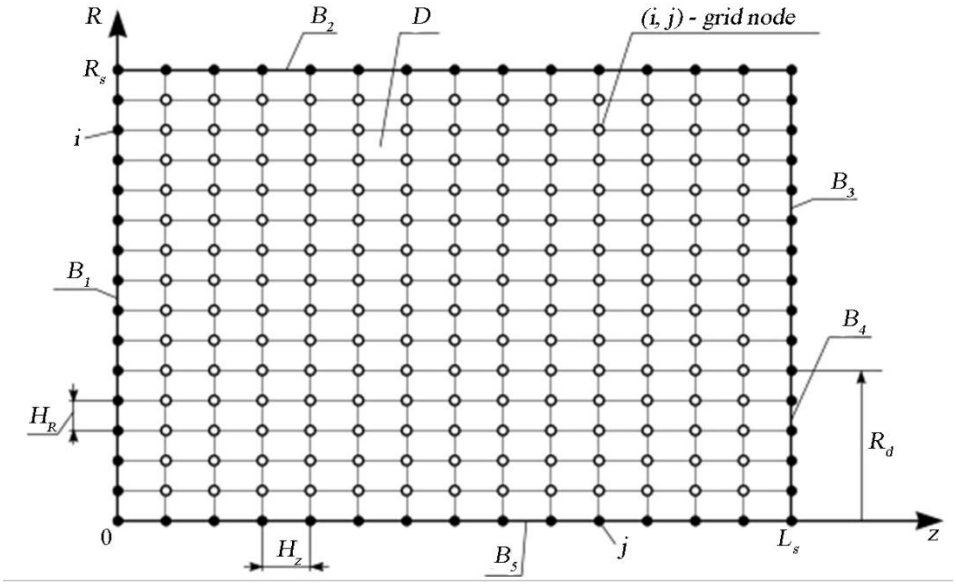


**Figure 5.** A grid model of domain D (CMD) for calculating melt flow near the die cavity: o–internal nodes; •-border nodes.

Let $r_d$ be the radius of a die cavity, and $l_c$, $r_c$ be the channel length and radius in the metering section. The radius of a die cavity $R_e$ was taken as an equivalent to $r_d$ in order to solve the problem:

$$R_e = r_d . \tag{49}$$

Thus, dimensionless geometry of a channel in the metering section can be found:

$$R_c = r_c / R_e, \quad L_c = l_c / R_e, \quad R_d = r_d / R_e. \tag{50}$$

For definiteness, let us assume that channel radius $r_в$ is tied to the radius of a die cavity: $r_в = K_R$

$r_м$, where $K_R$–integer (proportionality factor).

Let us determine the grid domain $D$:

$$D:\left\{Z_i=(i-1)H_z,\ R_j=(j-1)H_R),\ i=\overline{1,N_z}, j=\overline{1,N_R}\right\}, \tag{51}$$

Where:

$$H_z=L_в/n_z;\quad H_R=1/n_R;\quad N_z=n_z+1;\quad N_R=K_Rn_R+1, \tag{52}$$

Where: $n_z$–number of grid steps along the $Z$-axis; $n_R$–number of grid steps along the $R$-axis, divides channel radius.

Figure 2 shows boundaries of domain $D$, which may take the corresponding boundary conditions:

At $B_1$ –initial conditions (temperature, vorticity, and current);

At $B_2$, $B_3$ –first-order boundary conditions, conditions related to adhesion, or the lack of adhesion, at rheological melt/channel wall interface;

At $B_4$ –condition characterizing melt flow in the channel through the die;

At $B_5$ –starting point for setting symmetry conditions for flow parameters.

For discretisation, (35)–(38) were re-written as follows:

Equation for current function

$$\frac{\partial\overline{\omega}^*}{\partial\bar z}\frac{\partial\overline{\psi}}{\partial\bar r}-\frac{\partial\overline{\omega}^*}{\partial\bar r}\frac{\partial\overline{\psi}^*}{\partial\bar z}-\frac{\overline{\eta}}{Re}\left(\bar r\frac{\partial^2\overline{\omega}^*}{\partial\bar r^2}+\bar r\frac{\partial^2\overline{\omega}^*}{\partial\bar z^2}+3\frac{\partial\overline{\omega}^*}{\partial\bar r}\right)-\bar S_\omega=0, \tag{53}$$

Where:

$$\overline{\omega}^*=\overline{\omega}/\bar r; \tag{54}$$

energy equation

$$\frac{\partial\overline{\psi}}{\partial\bar r}\frac{\partial\overline{T}}{\partial\bar z}-\frac{\partial\overline{\psi}}{\partial\bar z}\frac{\partial\overline{T}}{\partial\bar r}-\varepsilon_r\left(\bar r\frac{\partial^2\overline{T}}{\partial\bar z^2}+\frac{\partial\overline{T}}{\partial\bar r}+\bar r\frac{\partial^2\overline{T}}{\partial\bar r^2}\right)-\bar r\overline{\Phi}=0, \tag{55}$$

Where: $\varepsilon_r=1/Pe;$

vorticity equation

$$\frac{\partial^2\overline{\psi}}{\partial\bar z^2}-\frac{1}{\bar r}\frac{\partial\overline{\psi}}{\partial\bar r}+\frac{\partial^2\overline{\psi}}{\partial\bar r^2}+\bar r^2\overline{\omega}^*=0, \tag{56}$$

Where: $\overline{\eta}$ is determined by (46), $\bar S_\omega$, $\overline{\Phi}$ –by (36) and (44), respectively.

Let us introduce the grid functions $\Omega_{ij}$, $\psi_{ij}$, *and* $\theta_{ij}$ into the (*i*, *j*) node (Figure 2) (functions correspond to $\overline{\omega}^*$, $\overline{\psi}_i$, *and* $\overline{T}$ ):

$$\Omega_{ij} = \overline{\omega}^*(Z_i, R_j); \quad \psi_{ij} = \overline{\psi}(Z_i, R_j); \quad \theta_{ij} = \overline{T}(Z_i, R_j); \tag{57}$$

$$A_{ij} = \frac{1}{Re}\overline{\eta}(\psi,\theta,Z,R,i,j); B_{ij} = \overline{S}_{\omega}(\psi,\theta,Z,R,i,j); C_{ij} = \overline{\Phi}(\psi,\theta,Z,R,i,j)R_j. \tag{58}$$

Below are designations for discretisation of derivatives:

$$D_z U_{ij} = \frac{u_{i+1,j} - u_{ij}}{H_z}, \; D_R U_{ij} = \frac{u_{i,j+1} - u_{ij}}{H_R} \text{ (right-hand differences)},$$

$$D_{\bar{z}} U_{ij} = \frac{u_{ij} - u_{i-1,j}}{H_z}, \; D_{\bar{R}} U_{ij} = \frac{u_{ij} - u_{i,j-1}}{H_R} \text{ (left-hand differences)}, \tag{59}$$

$$D_z U_{ij} = \frac{u_{i+1,j} - u_{i-1,j}}{2H_z}, \; D_R U_{ij} = \frac{u_{i,j+1} - u_{i,j-1}}{2H_R} \text{ (central differences)}.$$

For the second-order derivatives, expressions are the following:

$$D_{zz} U_{ij} = \frac{u_{i+1,j} - 2u_{ij} + u_{i-1,j}}{H_z^2}, \; D_{RR} U_{ij} = \frac{u_{i,j+1} - 2u_{ij} + u_{i,j-1}}{H_R^2}. \tag{60}$$

For mixed derivatives, designations are as follows:

$$D_{zR} U_{ij} = \frac{1}{H_z}\left(\frac{u_{i+1,j+1} - u_{i+1,j}}{H_R} - \frac{u_{i,j+1} - u_{ij}}{H_R}\right),$$

$$D_{z\bar{R}} U_{ij} = \frac{1}{H_z}\left(\frac{u_{i+1,j} - u_{i+1,j-1}}{H_R} - \frac{u_{ij} - u_{i,j-1}}{H_R}\right),$$

$$D_{zR} U_{ij} = \frac{1}{H_z}\left(\frac{u_{i+1,j+1} - u_{i+1,j-1}}{H_R} - \frac{u_{i,j+1} - u_{i,j-1}}{H_R}\right),$$

$$D_{\bar{z}R} U_{ij} = \frac{1}{H_z}\left(\frac{u_{i,j-1} - u_{ij}}{H_R} - \frac{u_{i-1,j+1} - u_{i-1,j}}{H_R}\right),$$

$$D_{\bar{z}R}U_{ij} = \frac{1}{H_z}\left(\frac{u_{i,j+1}-u_{i,j-1}}{2H_R} - \frac{u_{i-1,j+1}-u_{i-1,j-1}}{2H_R}\right),$$

$$D_{zR}U_{ij} = \frac{1}{H_z}\left(\frac{u_{i+1,j+1}-u_{i+1,j}}{H_R} - \frac{u_{i-1,j-1}-u_{i-1,j}}{H_R}\right),$$

$$D_{z\bar{R}}U_{ij} = \frac{1}{2H_z}\left(\frac{u_{i+1,j}-u_{i+1,j-1}}{H_R} - \frac{u_{i-1,j}-u_{i-1,j-1}}{H_R}\right),$$

$$D_{zR}U_{ij} = \frac{1}{2H_z}\left(\frac{u_{i+1,j+1}-u_{i-1,j-1}}{2H_R} - \frac{u_{i-1,j+1}-u_{i-1,j-1}}{2H_R}\right). \quad (61)$$

In (59)–(61), $u$ can take one of the following values, "$\Omega$", "$\psi$", *or* "$\theta$" ($u \in \{"\Omega","\psi","\theta"\}$).

Formula (61) is used to calculate $\bar{S}_{\omega}$.

With designations (57)–(61) given for internal nodes $\{i = \overline{2, N_z - 1},\ j = \overline{2, N_R - 1}\}$, Eqs (48)–(51) may be written as:

$$D_z\Omega_{ij}D_R\psi_{ij} - D_R\Omega_{ij}D_z\psi_{ij} - A_{ij}\left(R_j D_{RR}\Omega_{ij} + R_j D_{zz}\Omega_{ij} + 3D_R\Omega_{ij}\right) - B_{ij} = 0; \quad (62)$$

$$D_R\psi_{ij}D_z\theta_{ij} - D_z\psi_{ij}D_z\theta_{ij} - \varepsilon_r\left(R_j D_{zz}\theta_{ij} + D_R\theta_{ij} + R_j D_{RR}\theta_{ij}\right) - C_{ij} = 0; \quad (63)$$

$$\frac{1}{R_j}D_{zz}\psi_{ij} - \frac{1}{R_j^2}D_R\psi_{ij} + \frac{1}{R_j}D_{RR}\psi_{ij} + R_j\Omega_{ij} = 0. \quad (64)$$

Steady-state equations, such as (62)–(64), are solved using an interactive method [7,17], which requires the introduction of some definitions.

$\theta_{ij}$ is given at $B_1$, $B_2$. *and B3* (Figure 2):

$$\theta_{ij} = 1,\ (i,j) \in \{B_1 \cup B_2 \cup B_3\}, \quad (65)$$

Where: $\{B_1 \cup B_2 \cup B_3\}$– set of nodes of $B_1$, $B_2$ and $B_3$.

Let $\theta_{ij} be = 1$ in other points of a grid model, namely on the domain, including boundaries:

$$\theta_{ij} = 1 \text{ on } D \quad (66)$$

At channel inlet, boundary conditions are given as follows:

$$\psi_{1j} = R_j^2 \big/ 2;\ \Omega_{1j} = 0 \text{ at } B_2. \tag{67}$$

At channel border:

$$\psi_{iN_R} = 1/2 \text{ at } B_2. \tag{68}$$

$$\psi_{N_z j} = 1/2 \quad \text{at } B_3, \tag{69}$$

plus symmetry condition

$$\psi_{i1} = 0 \text{ at } B_5\,. \tag{70}$$

Let us assume

$$\psi_{ij} = R_j^2 \big/ 2 \tag{71}$$

in all internal points of *D*.

To determine the vorticity boundary conditions, boundary conditions for a vorticity function were approximated [14]:

$$\Omega_{1,j} = \frac{8\psi_{i,2} - \psi_{i,3}}{2H_R} \text{ at } B_5, \tag{72}$$

$$\Omega_{N_z j} = \frac{8\psi_{N_{z-2},\,j} - \psi_{N_{z-3},\,j}}{2H_z} \text{ at } B_3, \tag{73}$$

Let $\Omega_{ij} be = 0$ in all internal points of *D*.

At free boundary (at the channel exit, $B_4$):

$$\psi_{N_z\,j} = \psi_{N_{z-1},j};\ \Omega_{N_z\,j} = \Omega_{N_{z-1},j};\ \theta_{N_z\,j} = \theta_{N_{z-1},j}\,. \tag{74}$$

To solve (62)–(64), alternating direction method was used [9,14]. Let us explain its general structure on the example of two-dimensional operator steady-state equation

$$\Delta u = F\,. \tag{75}$$

Let us change (75) to non-steady-state equation

$$\frac{\partial u}{\partial \sigma} = \Delta u - F, \tag{76}$$

Where: $\sigma$-iteration parameter, analogous to time period. Below is the alternative directions scheme:

$$\frac{\tilde{u}_{ij} - u_{ij}}{\sigma_{zS}} = D_{zz}\tilde{u}_{ij} - D_{RR}u_{ij} - F_{ij}, \tag{77}$$

$$\frac{\hat{u}_{ij} - \tilde{u}_{ij}}{\sigma_{RS}} = D_{zz}\tilde{u}_{ij} - D_{RR}\hat{u}_{ij} - F_{ij}, \tag{78}$$

Where: $S$–iteration index; $\sigma_{RS}$, $\sigma_{zS}$–iteration parameters that differ in direction.

Thus, (75) was reduced to two tridiagonal systems of algebraic equations that can be solved by tridiagonal matrix algorithm. In (77) and (78), $\tilde{u} = u^{n+1/2}$, and $\hat{u} = u^{n+1}$, so at the first run, fractional solution $u^{n+1/2}$ is found and put in the second run (run in other direction) to find desired solution $u^{n+1}$.

With (77) and (78) in use, solution accuracy can be guided by the absolute criterion

$$max\left|\hat{u}_{ij} - u_{ij}\right| < \varepsilon, \tag{79}$$

or the fractional criterion

$$max\left|\frac{\hat{u}_{ij} - u_{ij}}{u_{ij}}\right| < \varepsilon_1. \tag{80}$$

Thus, solution accuracy depends on grid parameters $\sigma$ and $\varepsilon$. Experimental calculations confirm the existence of grid parameters that are close to those optimal for small Reynolds numbers. These parameters allow obtaining an approximate solution with the least time [14]. They are selected by computer-based experiments. There are methods for calculating the optimal set of parameters for some problems [14].

Let us write equations with the alternative directions for vorticity fields, current function and energy in the internal points of $D$.

I. System of vorticity Eq (7):

II.

$$\begin{aligned}\frac{\tilde{\Omega}_{ij}-\Omega_{ij}}{\sigma^{S}_{\Omega z}} &= D_z\tilde{\Omega}_{ij}D_R\psi_{ij}-D_R\Omega_{ij}D_z\psi_{ij}- \\ &-A_{ij}\left(R_j D_{RR}\Omega_{ij}+R_j D_{zz}\tilde{\Omega}_{ij}+3D_R\Omega_{ij}\right)-B_{ij}\end{aligned}, \tag{81}$$

$$\begin{aligned}\frac{\hat{\Omega}_{ij}-\tilde{\Omega}_{ij}}{\sigma^{S}_{\Omega R}} &= D_z\tilde{\Omega}_{ij}D_R\psi_{ij}-D_R\hat{\Omega}_{ij}D_z\psi_{ij}- \\ &-A_{ij}\left(R_j D_{RR}\hat{\Omega}_{ij}+R_j D_{zz}\tilde{\Omega}_{ij}+3D_R\hat{\Omega}_{ij}\right)-B_{ij}\end{aligned}, \tag{82}$$

Where: $\sigma^{S}_{\Omega z}$, $\sigma^{S}_{\Omega R}$–iteration parameters.

Equations (81) and (82), regrouped by transfer of unknown terms to the left, as well as known terms to the right, are as follows:

$$\frac{1}{\sigma^{S}_{\Omega z}}\tilde{\Omega}_{ij}-D_z\tilde{\Omega}_{ij}D_R\psi_{ij}+A_{ij}R_j D_{zz}\tilde{\Omega}_{ij}=W_{\Omega z_{ij}}, \tag{83}$$

$$\frac{1}{\sigma^{S}_{\Omega R}}\hat{\Omega}_{ij}+D_R\hat{\Omega}_{ij}D_z\psi_{ij}+A_{ij}\left(R_j D_{RR}\hat{\Omega}_{ij}+3D_R\hat{\Omega}_{ij}\right)=W_{\Omega R_{ij}}, \tag{84}$$

Where:

$$W_{\Omega z_{ij}}=\frac{1}{\sigma^{S}_{\Omega z}}\Omega_{ij}-D_R\Omega_{ij}D_z\psi_{ij}-A_{ij}\left(R_j D_{RR}\Omega_{ij}+3D_R\Omega_{ij}\right)-B_{ij}, \tag{85}$$

$$W_{\Omega R_{ij}}=\frac{1}{\sigma^{S}_{\Omega R}}\tilde{\Omega}_{ij}+D_z\tilde{\Omega}_{ij}D_R\psi_{ij}-A_{ij}R_j D_{zz}\tilde{\Omega}_{ij}-B_{ij}. \tag{86}$$

With (59)–(61), Eqs (83) and (84) may be written through $\Omega_{ij}$:

$$\frac{1}{\sigma^{S}_{\Omega z}}\tilde{\Omega}_{ij}+\frac{D_R\psi_{ij}}{H_z}\left(\tilde{\Omega}_{i+1,j}-\tilde{\Omega}_{ij}\right)+\frac{A_{ij}R_j}{H_z^2}\left(\tilde{\Omega}_{i+1,j}-2\tilde{\Omega}_{ij}+\tilde{\Omega}_{i-1,j}\right)=W_{\Omega z_{ij}}, \tag{87}$$

$$\frac{1}{\sigma_{\Omega R}^{S}}\hat{\Omega}_{ij}+\frac{D_z\psi_{ij}}{H_R}\left(\hat{\Omega}_{i,j+1}-\hat{\Omega}_{ij}\right)+\frac{A_{ij}R_j}{H_R^2}\left(\hat{\Omega}_{i,j+1}-2\hat{\Omega}_{ij}+\hat{\Omega}_{1,j-1}\right)+$$
$$+\frac{3A_{ij}}{H_R}\left(\hat{\Omega}_{i,j+1}-\hat{\Omega}_{ij}\right)=W_{\Omega R_{ij}} \tag{88}$$

or as a tridiagonal system of linear algebraic equations:

$$\alpha_{i-1,j}\tilde{\Omega}_{i-1,j}+\beta_{ij}\tilde{\Omega}_{ij}+\gamma_{i+1,j}\tilde{\Omega}_{i+1,j}=W_{\Omega z_{ij}}, \tag{89}$$

$$\alpha'_{i-1,j}\hat{\Omega}_{i,j-1}+\beta'_{ij}\hat{\Omega}_{ij}+\gamma'_{i,j+1}\hat{\Omega}_{i,j+1}=W_{\Omega R_{ij}}, \tag{90}$$

Where:

$$\alpha_{i-1,j}=\frac{A_{ij}R_j}{H_z^2};\ \beta_{ij}=\frac{1}{\sigma_{\Omega z}^{S}}+\frac{D_R\psi_{ij}}{H_z}-\frac{2A_{ij}R_j}{H_z^2};$$

$$\gamma_{i+1,j}=-\frac{D_R\psi_{ij}}{H_z}+\frac{A_{ij}R_j}{H_z^2}; \tag{91}$$

$$\alpha'_{i,j-1}=\frac{A_{ij}R_j}{H_R^2};\ \beta'_{ij}=\frac{1}{\sigma_{\Omega R}^{S}}-\frac{D_z\psi_{ij}}{H_R}-\frac{2A_{ij}R_j}{H_R^2}-\frac{3A_{ij}}{H_R};$$

$$\gamma'_{i,j+1}=\frac{D_z\psi_{ij}}{H_R}+\frac{A_{ij}R_j}{H_R^2}+\frac{3A_{ij}}{H_R}. \tag{92}$$

I. System of equations for vorticity function (64):

$$\frac{\tilde{\psi}_{ij}-\psi_{ij}}{\sigma_{\psi z}^{S}}=D_{zz}\tilde{\psi}_{ij}-\frac{1}{R_j}D_R\psi_{ij}+D_{RR}\psi_{ij}+R_j^2\Omega_{ij}, \tag{93}$$

$$\frac{\hat{\psi}_{ij}-\tilde{\psi}_{ij}}{\sigma_{\psi R}^{S}}=D_{zz}\tilde{\psi}_{ij}-\frac{1}{R_j}D_R\hat{\psi}_{ij}+D_{RR}\hat{\psi}_{ij}+R_j^2\Omega_{ij}, \tag{94}$$

Where: $\sigma_{\psi z}^{S}$, $\sigma_{\psi R}$–iteration parameters.

With unknown terms of (93) and (94) regrouped to the left and known terms regrouped to the right, transformation will be as follows:

$$\frac{1}{\sigma_{\psi z}^{S}}\tilde{\psi}_{ij} - D_{zz}\tilde{\psi}_{ij} = W_{\psi z_{ij}}, \tag{95}$$

$$\frac{1}{\sigma_{\psi R}^{S}}\hat{\psi}_{ij} + \frac{1}{R_j}D_R\hat{\psi}_{ij} - D_{RR}\hat{\psi}_{ij} = W_{\psi R_{ij}}, \tag{96}$$

Where:

$$W_{\psi z_{ij}} = \frac{1}{\sigma_{\psi z}^{S}}\psi_{ij} - \frac{1}{R_j}D_R\psi_{ij} + D_{RR}\psi_{ij} + R_j^2\Omega_{ij}, \tag{97}$$

$$W_{\psi R_{ij}} = \frac{1}{\sigma_{\psi R}^{S}}\tilde{\psi}_{ij} + D_{zz}\tilde{\psi}_{ij} + R_j^2\Omega_{ij}. \tag{98}$$

With (59)–(61), Eqs (95) and (97) may be written through $\psi_{ij}$

$$\frac{1}{\sigma_{\psi z}^{S}}\tilde{\psi}_{ij} - \frac{1}{H_z^2}\left(\tilde{\psi}_{i-1,j} - 2\tilde{\psi}_{i,j} + \tilde{\psi}_{i+1,j}\right) = W_{\psi z_{ij}}, \tag{99}$$

$$\frac{1}{\sigma_{\psi z}^{S}}\hat{\psi}_{ij} + \frac{1}{R_j H_R}\left(\hat{\psi}_{i,j+1} - \hat{\psi}_{i,j}\right) - \frac{1}{H_R^2}\left(\hat{\psi}_{i,j-1} - 2\hat{\psi}_{i,j} + \hat{\psi}_{i,j+1}\right) = W_{\psi R_{ij}} \tag{100}$$

or as a tridiagonal system of linear algebraic equations:

$$\alpha_{i-1,j}\tilde{\psi}_{i-1,j} + \beta_{ij}\tilde{\psi}_{ij} + \gamma_{i+1,j}\tilde{\psi}_{i+1,j} = W_{\psi z_{ij}}, \tag{101}$$

$$\alpha'_{i,j-1}\psi_{i,j-1} + \beta'_{ij}\psi_{ij} + \gamma'_{i,j+1}\psi_{i,j+1} = W_{\psi R_{ij}}, \tag{102}$$

Where:

$$\alpha_{i-1,j} = -\frac{1}{H_z^2};\ \beta_{ij} = \frac{1}{\sigma_{\psi z}^{S}} + \frac{2}{H_z^2};\ \gamma_{i+1,j} = -\frac{1}{H_z^2}; \tag{103}$$

$$\alpha'_{i,j-1} = -\frac{1}{H_R^2};\ \beta'_{ij} = \frac{1}{\sigma_{\psi R}^{S}} - \frac{1}{R_j H_R} + \frac{2}{H_R^2};\ \gamma'_{i,j+1} = -\frac{1}{R_j H_R} - \frac{1}{H_R^2}. \tag{104}$$

II. System of energy Eq (63):

$$\frac{\tilde{\theta}_{ij}-\theta_{ij}}{\sigma_{\theta z}^{S}}=D_R\psi_{ij}D_z\tilde{\theta}_{ij}-D_z\psi_{ij}D_R\theta_{ij}- \\ -\varepsilon_r\left(R_jD_{zz}\tilde{\theta}_{ij}+D_R\theta_{ij}+R_jD_{RR}\theta_{ij}\right)-C_{ij}, \tag{105}$$

$$\frac{\hat{\theta}_{ij}-\tilde{\theta}_{ij}}{\sigma_{\theta R}^{S}}=D_R\psi_{ij}D_z\tilde{\theta}_{ij}-D_z\psi_{ij}D_R\hat{\theta}_{ij}- \\ -\varepsilon_r\left(R_jD_{zz}\tilde{\theta}_{ij}+D_R\hat{\theta}_{ij}+R_jD_{RR}\hat{\theta}_{ij}\right)-C_{ij}, \tag{106}$$

Where: $\sigma_{\theta z}^{S}$, $\sigma_{\theta R}^{S}$–iteration parameters.

With unknown terms of (105), and (106) regrouped to the left, and known terms regrouped to the right, transformation will be as follows:

$$\frac{1}{\sigma_{\theta z}^{S}}\tilde{\theta}_{ij}-D_R\psi_{ij}D_z\tilde{\theta}_{ij}+\varepsilon_rR_jD_{zz}\tilde{\theta}_{ij}=W_{\theta z_{ij}}, \tag{107}$$

$$\frac{1}{\sigma_{\theta R}^{S}}\hat{\theta}_{ij}+D_z\psi_{ij}D_R\hat{\theta}_{ij}+\varepsilon_rD_R\hat{\theta}_{ij}+\varepsilon_rR_jD_{RR}\hat{\theta}_{ij}=W_{\theta R_{ij}}, \tag{108}$$

Where:

$$W_{\theta z_{ij}}=\frac{1}{\sigma_{\theta z}^{S}}\theta_{ij}-D_z\psi_{ij}D_R\theta_{ij}-\varepsilon_r\left(D_R\theta_{ij}+R_jD_{RR}\theta_{ij}\right)-C_{ij}, \tag{109}$$

$$W_{\theta R_{ij}}=\frac{1}{\sigma_{\theta R}^{S}}\tilde{\theta}_{ij}+D_R\psi_{ij}D_z\tilde{\theta}_{ij}-\varepsilon_rR_jD_{zz}\tilde{\theta}_{ij}-C_{ij}. \tag{110}$$

With (59)–(61), Eqs (109) and (110) may be written through $\theta_{ij}$

$$\frac{1}{\sigma_{\theta z}^{S}}\tilde{\theta}_{ij}-\frac{D_R\psi_{ij}}{H_z}(\tilde{\theta}_{i+1,j}-\tilde{\theta}_{ij})+\frac{\varepsilon_rR_j}{H_z^2}(\theta_{i+1,j}-2\theta_{i,j}+\theta_{i-1,j})=W_{\theta z_{ij}}, \tag{111}$$

$$\frac{1}{\sigma_{\theta R}^{S}}\hat{\theta}_{ij}+\frac{D_z\psi_{ij}}{H_R}(\hat{\theta}_{i,j+1}-\hat{\theta}_{ij})+\frac{\varepsilon_r}{H_R}(\hat{\theta}_{i,j+1}-\hat{\theta}_{ij})+$$

$$+\frac{\varepsilon_r R_j}{H_R^2}(\hat{\theta}_{i,j+1}-2\hat{\theta}_{ij}+\hat{\theta}_{i,j-1})=W_{\theta R_{ij}}, \tag{112}$$

or as a tridiagonal system of linear algebraic equations:

$$\alpha_{i-1,j}\tilde{\theta}_{i-1,j}+\beta_{ij}\tilde{\theta}_{ij}+\gamma_{i+1,j}\tilde{\theta}_{i+1,j}=W_{\theta z_{ij}}, \tag{113}$$

$$\alpha'_{i,j-1}\theta_{i,j-1}+\beta'_{ij}\theta_{ij}+\gamma'_{i,j+1}\theta_{i,j+1}=W_{\theta R_{ij}}, \tag{114}$$

Where:

$$\alpha_{i-1,j}=\frac{\varepsilon_r R_j}{H_z^2};\quad \beta_{ij}=\frac{1}{\sigma_{\theta z}^S}+\frac{D_R\psi_{ij}}{H_z}-\frac{2\varepsilon_r R_j}{H_z^2};\qquad \gamma_{i+1,j}=-\frac{D_R\psi_{ij}}{H_z}+\frac{\varepsilon_r R_j}{H_z^2}, \tag{115}$$

$$\alpha'_{i,j-1}=\frac{\varepsilon_r R_j}{H_R^2};\quad \beta'_{ij}=\frac{1}{\sigma_{\theta R}^S}-\frac{D_z\psi_{ij}}{H_R}-\frac{\varepsilon_r}{H_R}-\frac{2\varepsilon_r R_j}{H_R^2};\qquad \gamma'_{i,j+1}=\frac{D_z\psi_{ij}}{H_R}+\frac{\varepsilon_r}{H_R}+\frac{\varepsilon_r R_j}{H_R^2}. \tag{116}$$

## 3. Results and Discussions

In this article, a flow of a biopolymer melt is considered a continuous medium. The change in the viscosity of such an anomalously viscous and incompressible fluid is described by the rheological Eq (11) and the description is accurate enough. The Eq (11) is expressed as a generalized power law. This model is intended to describe the movement of a pseudo-plastic fluid the shear stress for which is a parameter defined by the power rheology law. For these pseudo-plastic fluids, viscosity decreases with the increase in the velocity gradient. The verification of obtained solution showed high adequacy: The resulting model allows calculating the flow rates of the rheological fluid melt in different sections near the die cavity with the accuracy sufficient for engineering calculations (± 10%). Therein, the viscosity of a rheological fluid η changes. It decreases by 7%.

The schemes of alternative directions were created to model vorticity fields (89–90), current function (99–100), and energy (113–114). These schemes were presented as a system of algebraic equations. For solving the problem, these equations must be supplemented with boundary conditions (67)–(74).

The problem of melt flow in the metering section was presented in the form of the finite-difference equations for vorticity, current function and energy (89), (90), (99), (100), (113), and (114). Because this problem is a large-scale problem, then solving it requires an iterative method or a sequence of steps.

To model the flow of a rheological melt, *Model 1* program was developed in *Turbo Pascal 7.0* under Windows 10. This program includes *Ris* and *Glob* modules.

The Glob module is designed to set constants and variables used in the program. The *Ris*

module is to display graphs on the monitor, namely, graphs of velocities along the channel axis in various cross-sections.

The key module, *Model 1*, calculates parameters of rheological melt flow in the metering section.

*Block 1* implies the initialization of variables and arrays, as well as the calculation of *Re, Pe,* $E_c$, $K_1$, criteria of a difference grid step. Initial values are assigned to grid functions.

At the iterative process start, temperature is assumed to be constant throughout the entire zone. The melt flows with initial velocity through the zone in a non-vortical motion, so the temperature was taken as

$$Q_{m_{ij}} = (Q_{wall} + Q_{inlet})/2,\ (i, j) \in D, \tag{117}$$

Where: $Q_{wall}, Q_{inlet}$ –temperature of channel wall and flow at the channel inlet, respectively;

vorticity as $O_{m_{ij}} = 0, (i, j) \in D,$

current as $F_{m_{ij}} = 0,\ (i, j) \in D.$

Calculation results from *model. rez* file were used as input data in subsequent modelling.

*Block 2* implies the calculation of melt flow rate at channel inlet, which result is assigned to a switching variable.

*Blocks* 3, 4, and 5 imply the melt flow determination. First, melt flow is determined in metering section, then vorticity and energy are determined. In any case, determination ends when accuracy criteria (79) and (80) are met at *Eps*=1·10$^{-6}$ and $\sigma_{\theta z} = \sigma_{\theta R} = 10000,$

$\sigma_{\Omega z} = \sigma_{\Omega R} = \sigma_{\varphi z} = \sigma_{\varphi R} = 1000.$

*Block* 6 implies the calculation of the volume rate of flow *Rashs* though the die cavity.

*Block* 7 implies the analysis of calculations: calculation either continues (return to Block 3), or is finished (move on to Block 8). Calculation is finished if the volume rate of flow through the die cavity overstrives that at the channel inlet.

*Block 8* implies the display of results on the monitor and the transfer of calculation results to the *model. rez* file. The velocity profiles for various sections of the channel are recorded in this file. The velocity profiles of various zones in the channel near the die cavity were displayed on the monitor.

**Table 1.** Initial data for calculation.

| parameter | unit of measurement | value |
|---|---|---|
| Die cavity radius | m | 0.0020 |
| Inlet radius | m | 0.0060 |
| Inlet length | m | 0.0120 |
| Equivalent radius | m | 0.0060 |
| Inlet temperature | K | 433.0000 |
| Channel wall temperature | k | 453.0000 |
| Air pressure | kPa | 101.3250 |
| Inlet velocity in z-direction | m/s | 0.0300 |
| Rheological equation: $\psi = 0$ | Pa/s | 220.0000 |
| Rheological equation: m-const | | 0.9800 |
| Rheological equation: beta–const | | 0.0020 |
| Heat conductivity of melt | W/(m·K) | 0.2200 |
| Specific heat capacity of melt | J/(kg·K) | 1600.0000 |
| Melt density | $kg/m^3$ | 1200.0000 |
| Temperature conductivity coefficient | $m^2/s$ | 11.600e-8 |
| Eckert's number | | 0.124e-8 |
| Reynolds number | | 98.182e-5 |
| Peclet number | | 1570.9091 |
| $K_1$ number* | | 25.0000 |
| z-coordinate increment | | 0.0270 |
| r-coordinate increment | | 0.0417 |

*Note: $K_1$–dimensionless criterion equal to the ratio between channel inlet radius $r_{inlet}$ and die outlet length l:*

$$K_1 = \frac{r_в}{l}$$

**Table 2.** Calculation results.

| Coordinate | Coordinate $Z = L/R_Э$ | | | | | |
|---|---|---|---|---|---|---|
| $R = r/R_Э$ | 0.7800 | 1.0500 | 1.3200 | 1.5900 | 1.8600 | 2.0000 |
| 0.000 | 1.6274 | 1.2378 | 0.7900 | 0.4262 | 0.1987 | 0.1701 |
| 0.042 | 3.2898 | 2.4797 | 1.5711 | 0.8411 | 0.3729 | 0.3086 |
| 0.083 | 4.9523 | 3.7217 | 2.3521 | 1.2560 | 0.5471 | 0.4471 |
| 0.125 | 5.5369 | 4.1380 | 2.6036 | 1.3838 | 0.5825 | 0.4630 |
| 0.167 | 5.8646 | 4.3486 | 2.7189 | 1.4357 | 0.5741 | 0.4331 |
| 0.208 | 6.0998 | 4.4771 | 2.7765 | 1.4544 | 0.5415 | 0.3685 |
| 0.250 | 6.2959 | 4.5634 | 2.8018 | 1.4540 | 0.4935 | 0.2644 |
| 0.292 | 6.4762 | 4.6244 | 2.8057 | 1.4408 | 0.4388 | 0.0987 |
| 0.333 | 6.6519 | 4.6678 | 2.7932 | 1.4181 | 0.3910 | 0.0000 |
| 0.375 | 6.8281 | 4.6966 | 2.7664 | 1.3873 | 0.3663 | 0.0000 |
| 0.417 | 7.0074 | 4.7121 | 2.7265 | 1.3494 | 0.3607 | 0.0000 |
| 0.458 | 7.1905 | 4.7140 | 2.6738 | 1.3046 | 0.3574 | 0.0000 |
| 0.500 | 7.3764 | 4.7011 | 2.6077 | 1.2529 | 0.3498 | 0.0000 |
| 0.542 | 7.5629 | 4.6712 | 2.5279 | 1.1942 | 0.3371 | 0.0000 |
| 0.583 | 7.7462 | 4.6216 | 2.4335 | 1.1283 | 0.3201 | 0.0000 |
| 0.625 | 7.9187 | 4.5477 | 2.3227 | 1.0547 | 0.2998 | 0.0000 |
| 0.667 | 8.0633 | 4.4402 | 2.1921 | 0.9721 | 0.2766 | 0.0000 |
| 0.708 | 8.1327 | 4.2746 | 2.0306 | 0.8760 | 0.2497 | 0.0000 |
| 0.750 | 7.9931 | 3.9816 | 1.8060 | 0.7525 | 0.2153 | 0.0000 |
| 0.792 | 7.2924 | 3.3796 | 1.4316 | 0.5636 | 0.1620 | 0.0000 |
| 0.833 | 5.2071 | 2.0434 | 0.7033 | 0.2191 | 0.0622 | 0.0000 |
| 0.875 | 0.0679 | -0.8862 | -0.7924 | -0.4637 | -0.1388 | 0.0000 |
| 0.917 | -10.9755 | -6.8679 | -3.7565 | -1.7952 | -0.5320 | 0.0000 |
| 0.958 | -31.8098 | -17.8692 | -9.1308 | -4.1914 | -1.2358 | 0.0000 |
| 1.000 | 0.0000 | 0.0000 | 0.0000 | 0.0000 | 0.0000 | 0.0000 |

Calculations were made for the rheological melt in a channel, which length was $L$ = 12 mm, which diameter was $D$ = 12 mm, and which die cavities had diameter (d) of 4 mm. The total number of difference grid nodes in $D$ was $N_{zR}$ = 1875. The number of nodes in z-direction was 75, in R-direction–25. The z-coordinate increment was $\Delta z = 0.027$, while the r-coordinate increment was $\Delta R = 0.0417$. The melt flow rate at channel inlet was Rashs = 0.0905 $m^3/s$, while at die cavity, it takes the value of Rashs = 0.0926 $m^3/s$, so the error is

$$\Delta = [(0.0905–0.0926)/0.0905]\cdot 100\% = 2.3\% \quad (118)$$

Viscosity profile of rheological fluid $\eta$ dropped from 265 to 248, down about 7%. Initial data and calculation results are given in Tables 1 and 2. Diagrams depicting velocities of rheological melt in various zones near the die cavity are shown in Figures 3 and 4.

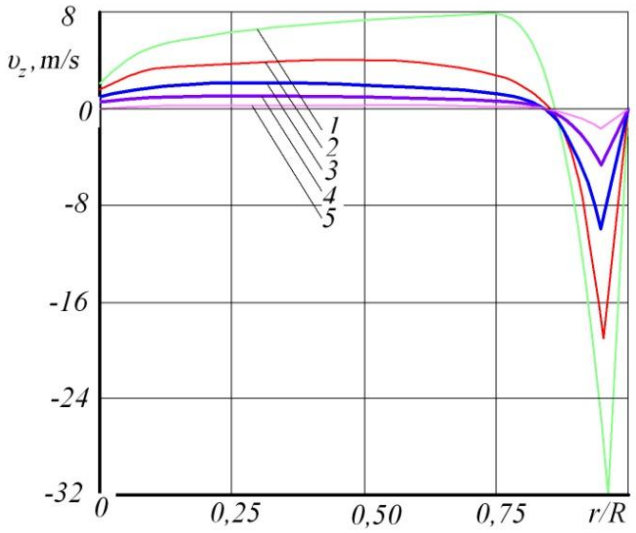


**Figure 6.** Flow velocity dependence on the relative radius in different cross-sections of the metering section (r/R): 1–2.00; 2–1.86; 3–1.9; 4–1.32; 5–1.05.

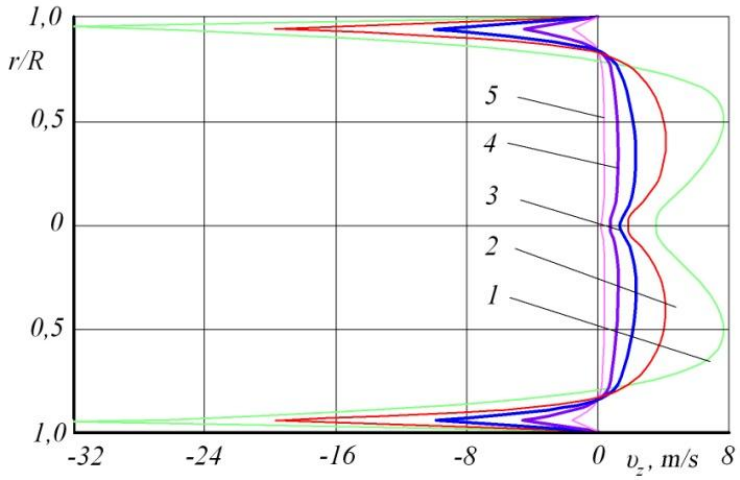


**Figure 7.** The flow velocity profiles of the channel inlet in different cross-sections of the metering section (r/R): 1–2.00; 2–1.86; 3–1.59; 4–1.32; 5–1.05.

Obtained model allows calculating the flow rate of rheological melt in various zones near the die cavity with sufficient accuracy (± 10%).

## 4. Conclusions

This article provides a mathematical model of non-isothermal rheological fluid in a cylindrical channel of a die. Computer testing verified the obtained solutions for the compliance with a real extrusion process. Results allow concluding a possibility of using the built-up model in matrix design for single-screw extruders [20–21]. The single-screw extruder is commonly used in polymer processing where the performance of the mixing section is significant in determining the quality of the final product. It is therefore of great interest to simulate the flow field in the single-screw extruder. The mixing performance of the extruder considerably influences the quality and morphology of the final product. For this reason, the flow field in the mixing section has been studied by a number of authors to gain a better understanding of the process. As an example of such work, you can give a link to the work [22]. Our work is different in that in the construction of our model we used more stringent boundary conditions, taking into account the biological nature of the polymer, implying the need for further use of the biopolymer extrudate as a food product.

## Acknowledgements

This article was done within the framework of 2018–2020 R&D project "Development of Technology for Pasta Production from Non-Traditional Poly-Grass Raw Materials" (State Registration Number 0118RK00310) funded by the grand of the Ministry of Education and Science of the Republic of Kazakhstan.

## Conflict of interest

All authors declare no conflicts of interest in this paper.

## References

1. L.G. Vinnikova, Extrusion processing of products with dietary fiber, *Food Ind.*, **11** (1991), 51–55.
2. A.N. Ostrikov, S.V. Shakhov, A.A, Ospanov, et al., Mathematical modeling of product melt flow in the molding channel of an extruding machine with meat filling feeding, *J. Food Process Eng.*, **41** (2018), e12874.
3. J.M. McKelvey, *Polymer processing, translated from English*, Khimiya Publishing House, (1965), 444.
4. M. Walter, *Extrusion dies for plastics and rubber: Design and engineering computations, translated from English*, Professiya Publishing House, (2007), 472.
5. I.R. Raupov and A.M. Shagiakhmetov, The results of the complex rheological studies of the cross-linked polymer composition and the grounding of its injection volume, *Int. J. Civil Eng. Tech.*, **10** (2019), 493–509.
6. A.N. Ostrikov, O.V. Abramov, V.N. Vasilenko, et al., *Mathematical modeling of anomalously viscous flow in the channels of extruders*, Publishing and Printing Center of Voronezh State University, (2010), 240.

7. A. Ospanov, L. Gaceu, A. Timurbekova, et al., *Innovative technologies of grain crops processing*, (2014), 439.
8. A.N. Ostrikov, O.V. Abramov and R. Nenakhov, *Patent 2142361 Russian Federation, Extrusion die with adjustable profile of a forming channel*. (Application No. 98118397). http://www1.fips.ru/fips_servl/fips_servlet?DB=RUPAT&DocNumber=2142361&TypeFile=html
9. A.N. Ostrikov, O.V. Abramov, R.V. Nenakho, et al., *Patent 2161556 Russian Federation, Extruder for the production of shaped article with adjustable profile of a forming channel* (Application No. 99114877). http://www1.fips.ru/fips_servl/fips_servlet?DB=RUPAT&DocNumber=2161556&TypeFile=html
10. V.P. Pervadchuk, N.M. Trufanova and V.I. Yankov, The mathematical model and numerical analysis of heat transfer processes involving polymer melting in plasticizing extruders, *J. eng. phy. thermophysics*, **1** (1985), 75–78.
11. V.V. Skachkov, R.V. Torner, Yu.V. Stungur, et al., *Modeling and optimization of polymer extrusion, Chemistry*, Khimiya Publishing House, (1984), 152.
12. T. Zehev and C.G. Gogos, *Principles of Polymer Processing, 2nd Edition*, John Wiley & Sons, (2013), 624.
13. R.V. Torner, *Theoretical bases of polymer processing*, Khimiya Publishing House, (1977), 460.
14. D.H. Chang, *Rheology in polymer processing*, Khimiya Publishing House, (1979), 368.
15. V.I. Yankov, V.I. Pervadchuk and V.I. Boyarchenko, *Processing of Fiber-Forming Polymers*, Khimiya Publishing House, (1989), 320.
16. C. Rauwendaal, *Polymer extrusion*, (1990), 568.
17. M. Kristiawan, L. Chaunier, G. Della Valle, et al., Modeling of starchy melts expansion by extrusion, *Trends food sci. technol.*, **48** (2016), 13–26.
18. J.M. Bouvier and O.H. Campanella, *Extrusion processing technology: Food and non-food biomaterials*, John Wiley & Sons, (2014).
19. L. Chaunier, S. Guessasma, S. Belhabib, et al., *Material extrusion of plant biopolymers: Opportunities & challenges for 3D printing*, (2017).
20. Q.T. Ho, J. Carmeliet, A.K. Datta, et al., Multiscale modeling in food engineering, *J. food Eng.*, **114** (2013), 279–291.
21. K. Lamnawar, A. Maazouz, G. Cabrera, et al., Interfacial tension properties in biopolymer blends: From deformed drop retraction method (DDRM) to shear and elongation rheology-application to blown film extrusion, *Int. Polymer Process*, **33** (2018), 411–424.
22. J.M. Buick, Lattice Boltzmann simulation of power-law fluid flow in the mixing section of a single-screw extruder, *Chem. Eng. Sci.*, **64** (2009), 52–58.